

# A Study of the hydrogeological environment of the lishan landslide area using resistivity image profiling and borehole data

Cheng-Chao Lee <sup>a,\*</sup>, Chieh-Hou Yang <sup>b</sup>, Hsing-Chang Liu <sup>a</sup>,  
Kuo-Liang Wen <sup>a</sup>, Zi-Bin Wang <sup>b</sup>, Yi-Jie Chen <sup>b</sup>

<sup>a</sup> *Institute of Geophysics, National Central University, Taiwan, ROC*

<sup>b</sup> *Department of Engineering, Ching-Yun University, Taiwan, ROC*

Received 15 December 2006; received in revised form 8 January 2008; accepted 20 January 2008

Available online 13 February 2008

## Abstract

Resistivity Image Profiling (RIP) surveys was used to develop a lithological and hydrogeological model of the subsurface in the southeastern part of Lishan landslide area of central Taiwan. The bedrock consists of slate in the study area. Based on RIP and rock samples collected from boreholes results, three electrical strata are recognized: colluvium, the shear zone composed of shear gouges and shattered slate, and the undisturbed slate formation. The steep shear zone with resistivity ranging between 100~260  $\Omega$ -m, plays a crucial role in the local hydrogeological environment, because it forms a natural barrier which blocks and retains groundwater flowing down the slope. Groundwater will brim over the barrier when the water level is high. Thus the inclined groundwater table remains stable from long-term monitoring. It strongly indicates that the groundwater recharge is greater than that of discharge. Therefore, the shear zone can provide information about the optimum locations for draining the excess groundwater in-situ for slope stability consideration.

The curved basal surface of the colluvium and the weathered slate can also be discerned from the resistivity variations and boreholes data. A series of circular patterns may associate with the main slope failure which migrated upwards from the lower slope.

© 2008 Elsevier B.V. All rights reserved.

*Keywords:* Landslide; Groundwater; Resistivity; Shear zone

## 1. Introduction

The Lishan landslide area is located in central Taiwan, at the intersection of the East-West Cross-Island Highway Route 8 and Highway Route 7A (Fig. 1). Lishan has a distinctive climate and flourishing agriculture. In mid-April 1990, incessant downpours caused a landslide on the downslope of the Lishan Grand Hotel and Highway Routes 7A and 8; traffic was interrupted and buildings were badly damaged.

Previous reports (ITRI, 1993; CECI, 1997) indicate that the displacement of the slip surface was closely related to intense precipitation. A mitigation project from 1995 to 2003 involved the construction of ditches to lower groundwater levels and collect surface water. This main subsurface drainage construction (Fig. 2)

included 15 sets of drainage wells 3.5 m in diameter and ranging from 15 to 40 m in depth. It also included Gallery G1, 350 m in length and equipped with 4863 m of water collecting pipes, as well as Drainage Gallery G2, 550 m in length and equipped with 10,700 m of water collecting pipes. In addition, this project built 8 sets of automated monitoring systems with piezometers, inclinometers, and tiltmeters (SWCB, 2003). These facilities allowed the drainage gallery to discharge water at a maximum efficiency of 1000 l/min. It did lower the groundwater level below the elevation of the drainage gallery. The cost of mitigation project is more than US\$30 million.

Remedial construction for groundwater flow in the landslide area was subjected to several downpours and earthquakes (including the 1999 Chi-Chi Earthquake,  $M_L = 7.3$ ) but did not sustain major damage. The efficiency of the remediation was greater than anticipated by the original design (SWCB, 2003). Nevertheless, the groundwater level of the B-13 automated

\* Corresponding author.

E-mail address: [lcc@sinogeotech.com.tw](mailto:lcc@sinogeotech.com.tw) (C.-C. Lee).

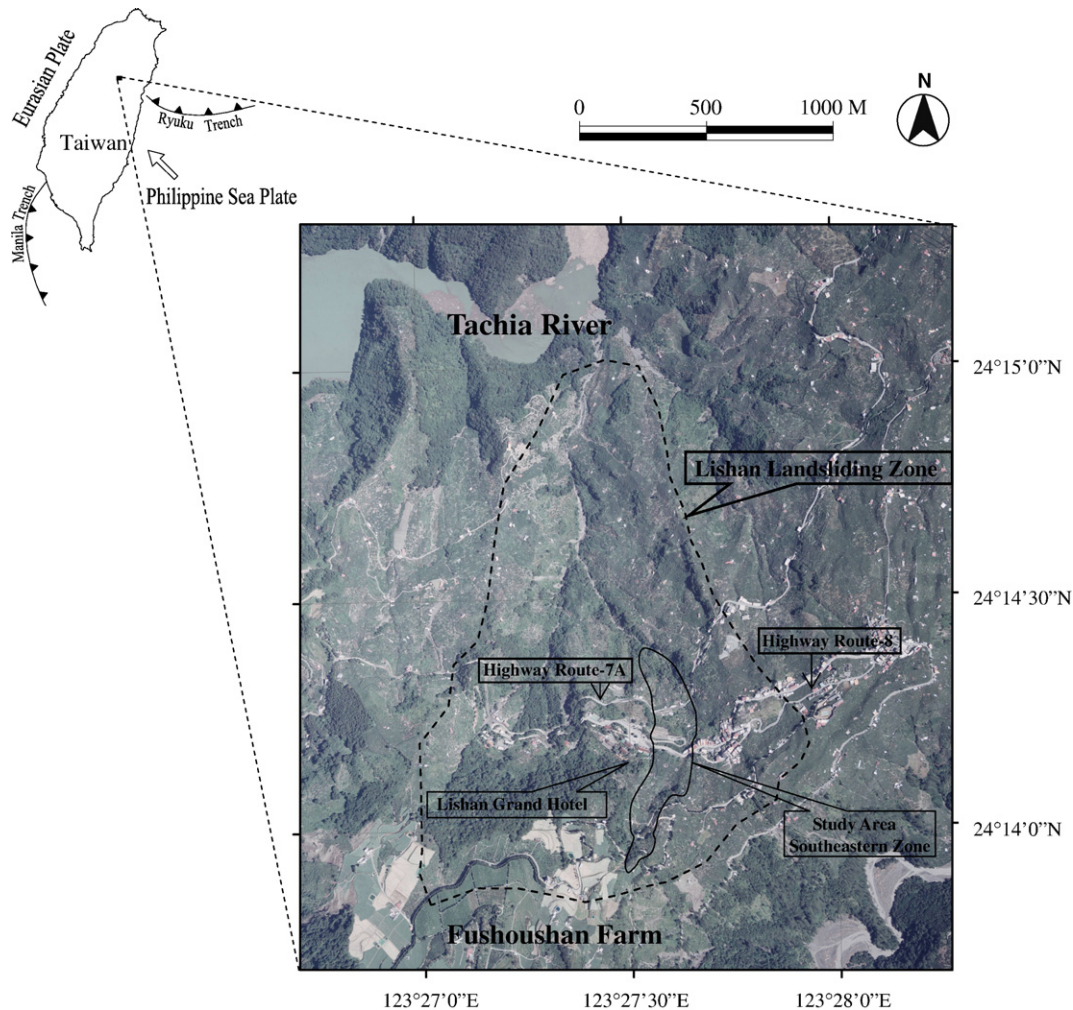


Fig. 1. Location map of the Lishan landslide area.

monitoring station (including well B-13, B13-OW1 and B13-OW2) in the southeast region (Fig. 2) has remained stable since the mitigation project started (Fig. 3). The mitigation had little to do with the groundwater level around B-13 automated monitoring station. In order to examine the abnormal character of the groundwater at well B13-OW1, water was continuously injected into the well at a rate of 50 liter/min. The groundwater level rose from GL.-25.8 m to a constant level of GL.-23.3 m. After stopping injection, the water level dropped from GL.-23.3 m to GL.-25.8 m within a few seconds. This indicates that the well has no clogs. The accumulation of groundwater around the B-13 automated monitoring station may be blocked by a barrier formed by lithological change, especially in the downslope direction. Fig. 3 shows that the groundwater level of well B-11 has larger variations than those shown in the station B-13, and it may be associated with rainfall. The well B-9 is in the north of well B-11 and has a lower topography. Its groundwater level is highly related to precipitation.

For an engineering purpose, most studies have stressed the distribution, composition, and mechanism of slipping bodies in the vicinity of the Highway Route 8 and Highway Route 7A. The landslide phenomenon was manifested in colluvial soils and the interface between colluvial soils and fractured slate or

undisturbed slate formations (Su et al., 1990). The colluvial soils consist of different clayey minerals which increase the instability of soils (Wan, 1986), whereas the slip surface consist of weak silty soils. All evidences indicate that the groundwater is one of the most important factors associated with instability of slopes. However, no literature discussed the lithological variation of rock and the groundwater system in-situ.

Borehole sampling and geophysical surveys are the best ways to study landslides. Borehole sampling serves as a direct observation. However, it provides only the well data. Connecting a limited number of lithological logs, especially in a rough terrain may not accurately reflect the correct subsurface conditions. Due to a limit depth of penetrating and heavy attenuation of the signal of weighting drop, collecting the seismic data is poor or unavailable on the dry and loose colluvium surface (ITRI, 1993). The RIP is a relatively cheap method to give a continuous subsurface image. Since the RIP method is sensitive to the water content of layers, it is suitable to be used in hydrogeological studies (Turesson, 2006; Nascimento et al., 2004; Šumanovac and Weisser, 2001; Šumanovac, 2006; Porsani et al., 2005; Gautam et al., 2000; Karastathis et al., 2002; Yaramanci, 2002) and landslide investigation (Lapenna et al., 2004; Mauritsch et al., 2000; Perrone et al.,

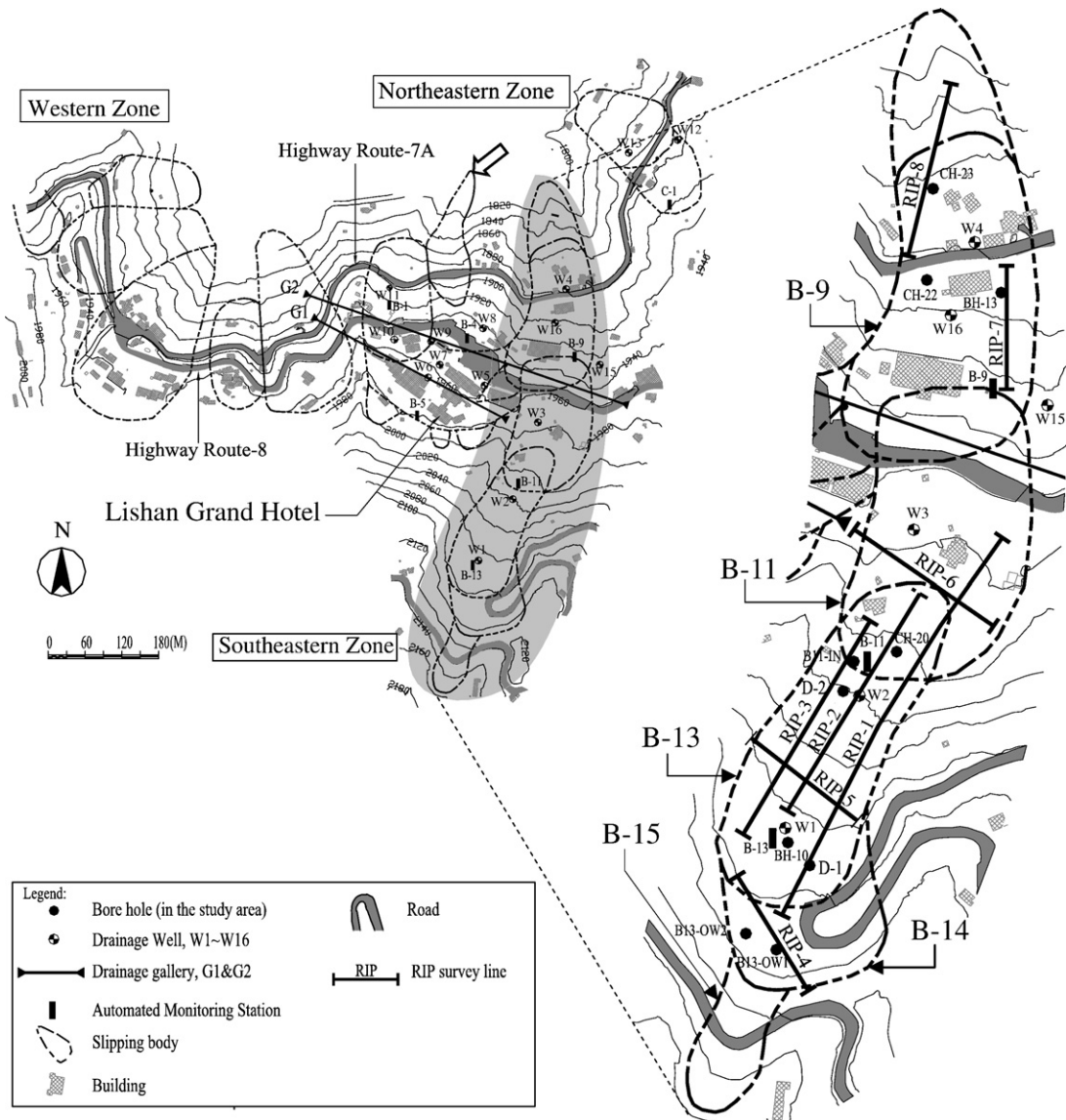


Fig. 2. Location map of slipping bodies, major subsurface drainage constructions, boreholes, and RIP survey lines. The blank arrow indicates landsliding body which occurred in mid-April 1990.

2004). Combining both RIP and borehole data may provide a better lithological and hydrogeological investigation of the study area.

## 2. Geological Setting

Taiwan is located along the oblique collision zone between the Philippine Sea plate and Eurasian plate (Fig. 1). It is widely believed that the mountain-building process is still in progress (Tsai et al. 1981; Yu and Chen 1994; Yu et al. 1999). The Lishan landslide area is in the west flank of Taiwan's Central Mountain Range, the elevation ranges from 1800 to 2100 m. The slope dips to the north and Fushuoshan Farm stands as the highest point to the south. Tachia River settles to the north of the farm. The study area is situated on an old landslide. The suspected major scarp of the Lishan landslide area can be observed from the southern side of the Lishan Grand Hotel (Fig. 4). In light of topography, geological surveys, and features of the landslide, the landslipping

area can be divided into three groups: western, southeastern, and northeastern (ITRI, 1993; CECI, 1997) (Fig. 2). Each zone is composed of a certain number of slipping bodies. The southeastern zone was chosen as the study site for the pilot project. Its dominant slipping direction is N-NE. Each slipping body in southeastern zone have a horseshoe-like surface shape whose width and length range from 80 to 200 m (Fig. 2).

Most of the bedrock in the Lishan landslide area is composed of slate of the Miocene Lushan Formation (Ho, 1986). Due to the monotonous lithology, it is unsuitable as a key bed to analyze geological structure patterns. Statistical analysis indicates that the schistosity of the slate is dominant in the N36°E/32°SE direction, which is nearly parallel to the slipping direction of the southeastern zone (CECI, 1997). The slate is affected by water, temperature, and organic activity. The weathered slate tends to disintegrate along the schistosity. Slaty fragment and clayey soils form the poorly cohesive colluvium.



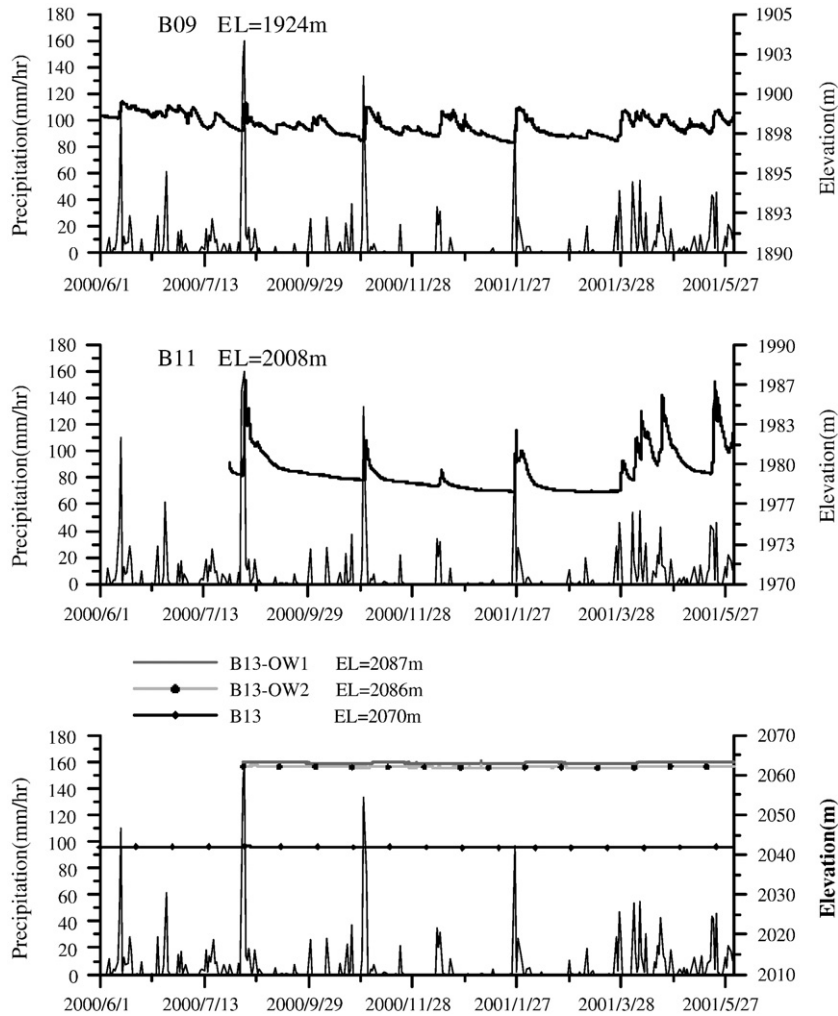


Fig. 3. Relation between hourly records of precipitation and groundwater level from B09, B11, and B13 automated monitoring stations.

The geological data obtained from old boreholes and drainage galleries indicate that the shear zones, composed of shear gouges and shattered slate, have different sizes (from centimeters to tens of meters in width) and high dip distribution, which may be highly related to tectonic movement (Sino Geotech, 2001, 2003). Due to variable width of the shear zone, it is difficult to correlate, even between the adjacent boreholes at short distance. So, the direction and extent of the shear zone still were not well defined from previous data in the Lishan landslide area. Formal geological investigations and mitigation of drainage ultimately provides only partial information on the geological structure pattern of the site.

### 3. RIP Data Acquisition

The RIP method was developed to elucidate complex subsurface structures (Griffiths and Barker, 1993). High-definition pseudosections were quickly obtained by dense sampling of apparent resistivity variation at shallow depths. Resistivity data was acquired by using Sting R1/IP manufactured by AGI, USA with a pole-pole array, which has the widest horizontal coverage and the deepest depth of investigation (Loke, 2001). This method

facilitates detailed, direct, and inverse interpretation of 2D resistivity distribution in the subsoil (Loke and Barker, 1996). A series of RIP lines were placed on the slipping body (Fig. 2). During the measurements taken for this study, two distant stationary electrodes were positioned at a distance ten times the

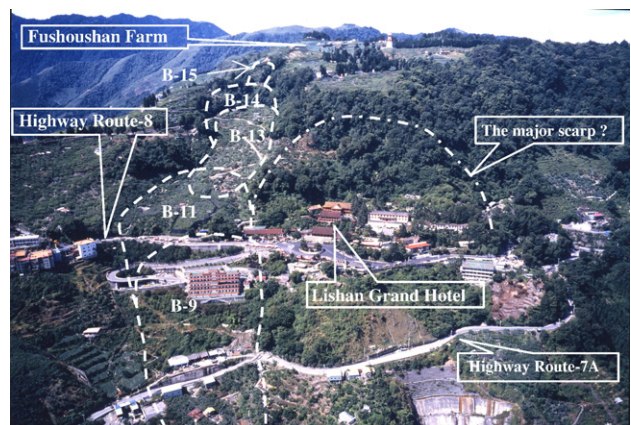


Fig. 4. A bird's eye view looking southward at the southeastern zone of the Lishan landslide area.

expected depth of exploration from the survey line. One electrode was a remote current electrode and the other was a remote potential electrode. Measurements were taken from both ends of the survey line, and involved a series of equally spaced electrodes. One of the end electrodes first served as a current electrode and the rest of the electrodes served as “roll along” potential electrodes. The resistivity response was computed from the fixed current electrode followed by a moveable potential electrode in the traverse position in sequential order. With each successive measurement, distance between the pair of electrodes was increased by an electrode’s spacing of 4~10 meters. Measurements were taken continuously until the maximum spacing had been reached. The current electrode was then shifted forward to the next location, the nearest potential electrode of the former current electrode. Pole-pole profiling measurement was taken from this new current electrode as the previous procedure. Measurements were repeated for each successive current electrode until the current electrode was moved to the location of the next farthest potential electrode (Fig. 5). The apparent resistivity measurements were inverted to obtain true resistivity structure by using a commercial RES2DINV. This resistivity software was based on 2.5D smoothness-constrained inversion, employing a quasi-Newtonian technique to reduce numerical calculations (Loke and Barker, 1996). The final geoelectrical models show a root mean square(rms) error of 5.2~8.9 percent after five iterations.

#### 4. RIP Results

In order to avoid interruptions incurred by human-made facilities, all survey lines were deployed within the orchard (Fig. 2). In order to give a better correlation between the lithology and the measured resistivity, the resistivity of outcrops was measured in-situ.

The resistivity of the colluvium outcrops ranged from 13 to 324  $\Omega$ -m (Table 1) which were affected by the following factors:

1. Size of slate fragments: the size of slate fragments ranged from centimeters to tens of centimeters. The greater the size

Table 1

The resistivity of the slate and colluvium measured in the Li-Shan area

Sample	Lithology	Resistivity ( $\Omega$ -m)
1	Yellowish-grey to grey slate, light to medium weathering	173.8-252
2	Slightly damp colluvial soils	111.4
3	Yellowish-grey to dark grey slate, light to medium weathering, percolating water	55.8
4	Wetting more clayey colluvial soils	13.8
5	Light weathering and very dry slate	1321
6	Colluvial soils with much dry rock	255.9

and amount of fragments, the higher the resistivity of the colluvium will be.

2. Water content: higher water content will lead to the lower resistivity of the colluvium.
3. Content of fine-sized grains: the greater content of fines, the lower resistivity of the colluvium will be.

The resistivity of the slate outcrop ranged from 55 to 1321  $\Omega$ -m (Table 1). This depended on the following factors:

1. Clay and water content: the slate contains schistosity and irregular parting, which may be filled in by water and/or clay. This filling material will lead to the lowering of resistivity. Furthermore, this lowering resistivity effect is even more prominent for clay than water.
2. Degree of weathering: highly weathered slate exhibits lower resistivity.
3. Content of shear zone: The shear gouge and shattered slate in the shear zone will reduce the resistivity of the slate. The lithological data of the shear zone collected inside the drainage gallery indicates that the fresh rock sample was well-consolidated and dense, such as cemented breccia. The resistivity of the shear zone was lower than unweathered slate with less shear gouge content, but higher than that of water saturated colluvium and weathered slate.

The highest resistivity value shown in the RIP sections (Fig. 6) was less than 340  $\Omega$ -m. It indicates that there was no intact and dry slate in the RIP sections. An irregular and relatively high resistivity zone ( $>120$   $\Omega$ -m) was detected near the surface and it may associate with a high porosity and low moisture content of colluvium. The RIP-3 section shows that two relatively high resistivity zones ranging from 100 to 220  $\Omega$ -m at positions 20~60 m and 120~160 m were located below the colluvium with a steep distribution. Data obtained from the B11-1N borehole located in the high resistivity zone indicates that the depth of the basal colluvium was about 16 m below the surface, a fractured slate mingled with pervasive and considerable quantities of shear gouges was also found. Similar results can also be recognized in the adjoining survey lines RIP-1 and RIP-2 (Fig. 6), except having different ranges. The high resistivity zone shown in the RIP-1 section is at positions 190 and 230 m and that of the RIP-2 section has camel-back shape between positions 95 and 175 m. An extensive shear zone

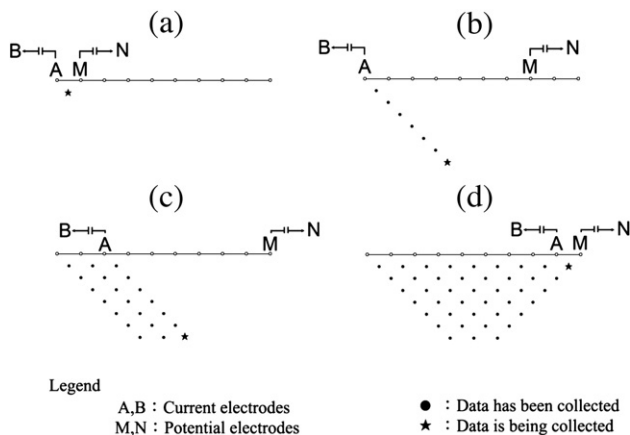
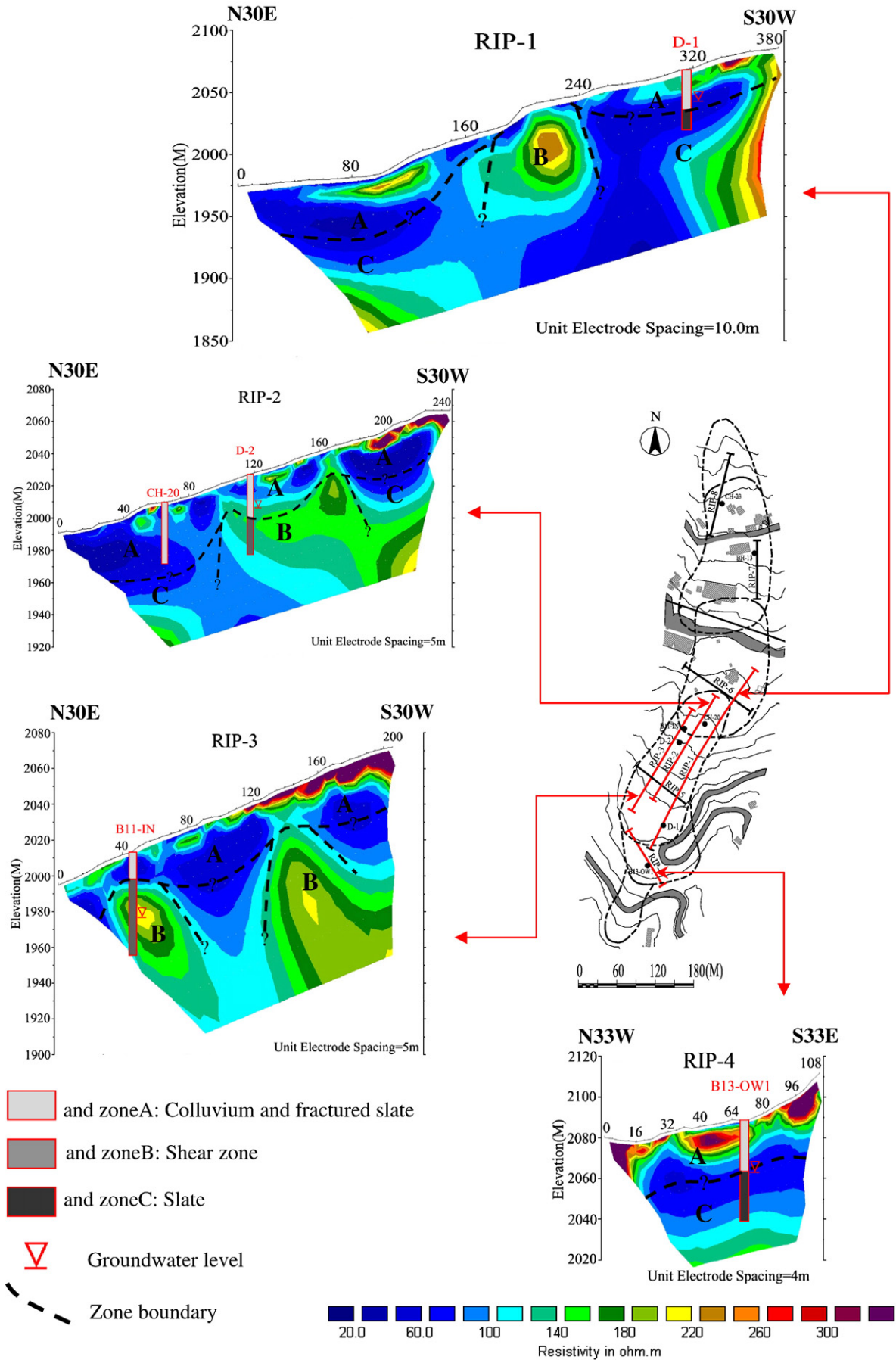


Fig. 5. Procedure of RIP survey using a pole-pole array.





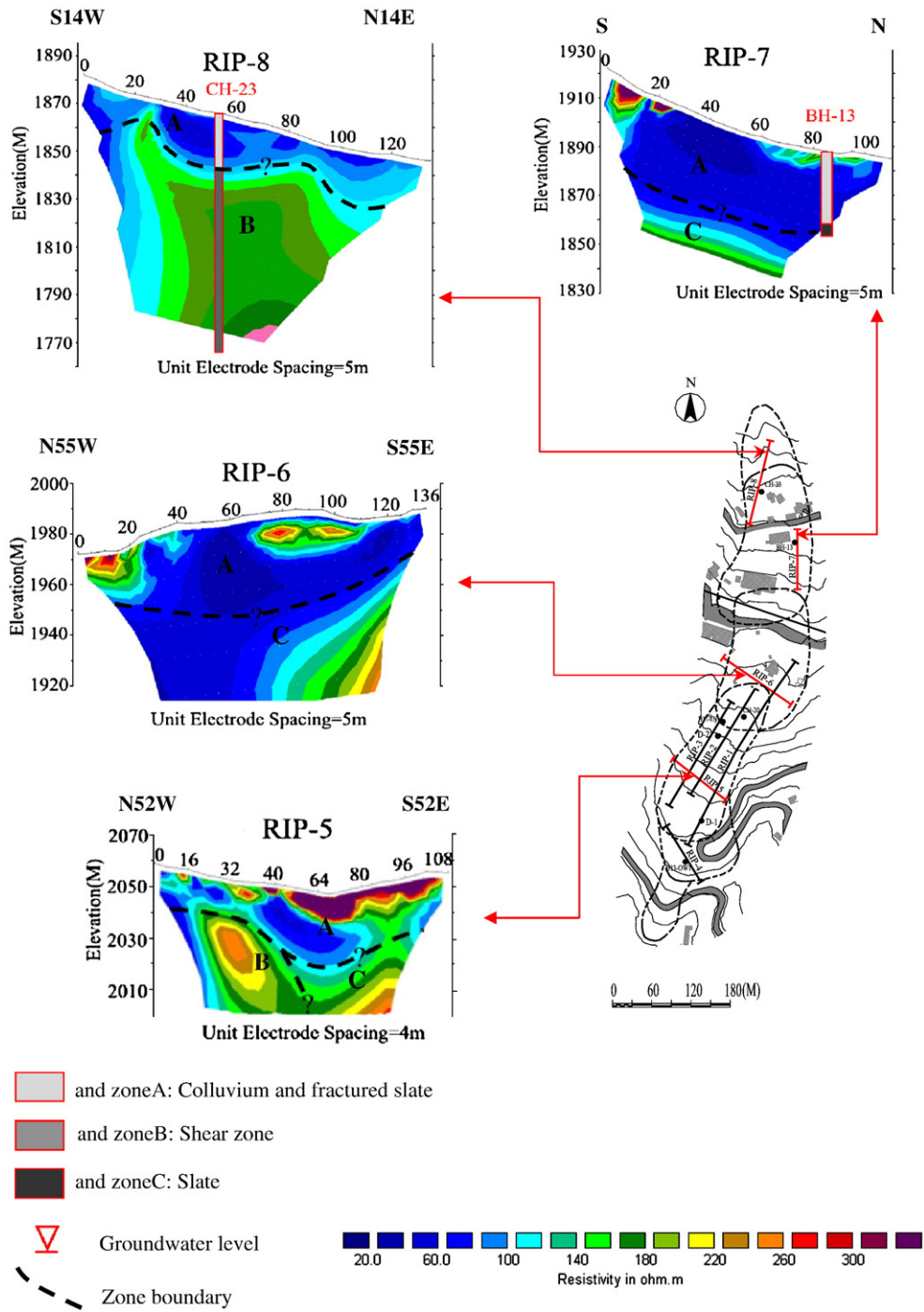


Fig. 6. Comparison between RIP and direct results.

identified by a previous borehole data (CH-23) matched well with the relatively high resistivity zone (100~260Ω-m) shown in the RIP-8 section (Fig. 6).

The iso-resistivity color bands of the shear zone on the left corner of RIP-3 section show a concentric ellipse. The groundwater level of borehole B11-1N remains at 1978 m a.s.l chronically within the shear zone. Therefore the resistivity between the top of shear zone and groundwater level in Borehole B11-1N increased gradually with depth. Below the groundwater level, the resistivity of the shear zone de-

creased as the depth increased. A similar type of resistivity distribution was recognized in the middle of the resistivity section of RIP-1.

The shear zone in the middle of the resistivity section of RIP-1 can be grouped to two low resistivity (less than 60 to 80 Ω-m) zones. The BH-12 borehole data indicates that the thickness of the colluvium was greater than 38 m. These two low resistivity zones may be associated with a saturated clay-rich colluvium. The RIP-6 section crossed the landsliding direction and in a relatively flat region. A wider and deeper low resistivity zone shown in RIP-6

section may be associated with a moist colluvium rich in clayey soils.

A layered pattern of the resistivity distribution shown in the RIP-4 section is comparable to that of borehole B13-OW-1. The groundwater level remained chronically around 2063 m a.s.l. The dry colluvium near the surface had a resistivity greater than 140  $\Omega$ -m. The clay-rich colluvium above the groundwater level has a resistivity lower than 100  $\Omega$ -m. Samples obtained from borehole B13-OW-1 indicate that the slate layer has low clay content (<10%) and well developed schistosity. Therefore, the resistivity increased as the depth increased from 25 m to 30 m, it is quite similar to that shown in RIP-7 section.

RIP-5 section was laid across the flow direction of the landslide. A bowl-shaped low resistivity zone between sounding locations 35 and 80 m was discerned. Its depth ranged from 25 to 30 m and may be associated with a mixture of clayey soils, wet colluvium, and moisty weathered slate. The relatively high resistivity zone in the western part of the section is comparable to the shear zone shown in RIP-3 section; the high resistivity zone near the surface is interpreted to be dry colluvium.

Resistivity patterns may be used to discern an undisturbed slate from shear zone. If the iso-resistivity color bands are nearly horizontal and parallel to the surface, it is more likely to be an undisturbed slate, as indicated by RIP-4 and RIP-7 sections. If the iso-resistivity color bands has a severe tilt, it may be related to a shattered slate and shear gouge, as indicated by RIP-3 and RIP-8 sections.

## 5. Validation of RIP Results

The distribution and appearance of shear zones in RIP-1, RIP-2, and RIP-3 sections are quite different. Only Borehole B11-1 N is located in these zones. Based on RIP results, two boreholes, D-1 and D-2 (Figs. 2 and 7), were selected and drilled. The maximum depth of both boreholes was 50 m.

### 5.1. Borehole D-1

The colluvium ranged from surface to GL-23.55 m, composed of grey slaty fragments and yellowish-brown sand-clay mixture. The slate ranged from GL-23.55 to GL-50 m, mixed with clay than 5 cm in thickness except for the interval between GL-30 to GL-32.5 m. The well developed schistosity shows an angle around 25 to 30 degrees in the slate. The groundwater level in the slate was 27.1 m below the surface. Comparison made between the RIP-1 section and lithology of borehole D-1 indicates that the shallow dry loose colluvium had a resistivity greater than 120  $\Omega$ -m. At the depth between GL-20.3 to GL-32.5 m a lot of clay exhibited low resistivities. Below the depth of GL-32.5 m, moisty weathered slate shows a slowly increasing resistivity with depth.

### 5.2. Borehole D-2

At the elevation above GL-27.8 m, the colluvium consists of yellow to grey slaty fragments, silty sand, and clay. Rock embedded grey charcoal shattered slate and shear gouge ranged from

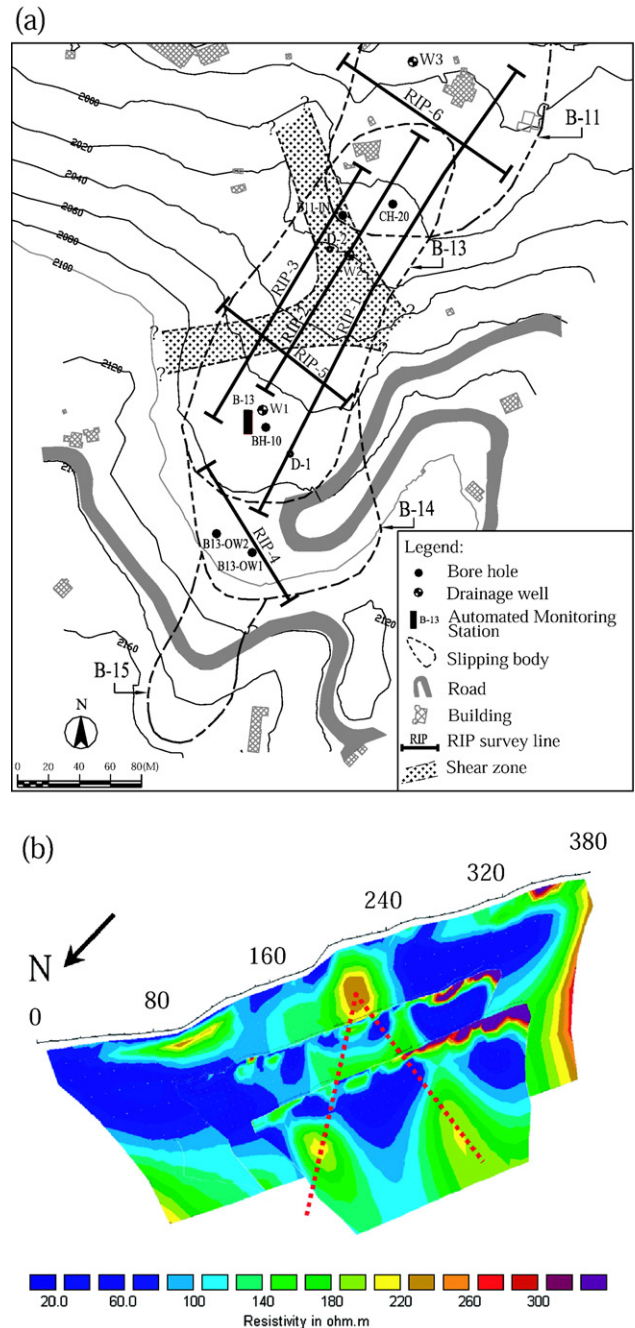


Fig. 7. Distribution of the shear zone. (a) A plane view (b) Viewed from RIP section in a W-E direction. The red dashed lines represent extending direction of the shear zone.

GL-27.8 to GL-50 m. Therefore the borehole was in a shear zone. The groundwater level within the colluvium was GL-21.6 m. Comparison made between the RIP-2 section and the lithology of the borehole indicates that the resistivity of the colluvium ranged from 60 to 100  $\Omega$ -m and resistivity of the shear zone ranged from 100 to 160  $\Omega$ -m.

## 6. Discussion

RIP results indicate that two strata had resistivities ranging from 50 to 80  $\Omega$ -m; for a moist clayey colluvium and a moist



weathered slate, respectively. Even though the depth of the basal colluvium could not be recognized precisely from RIP profiles, the shape of the colluvium can still be discerned from the resistivity variations. The resistivity sections of RIP-1 and RIP-2 suggest that the thickest colluvium at the lower part (north side) was quite similar to that of RIP-6.

The shear zone was formed by sheared slate, it contains considerable amount of clay/silt and has the permeability lower than the colluvium or weathered slate. A Lugeon test was carried out at a depth of 30~35 m in the borehole D-2. The Lugeon value is 7 and corresponds to a permeability of  $7 \times 10^{-5}$  cm/sec. The shear zone can be taken as a semipervious layer in this hydrogeological environment. The resistivity of shear zones below the groundwater tends to increase with depth; RIP-2 and RIP-3 sections exemplify this tendency. However, in the middle part of section RIP-1, the shear zone decreases its resistivity with depth (Fig. 6) below 1990 m a.s.l. The limited overburden above the shear zone results in the releasing of pressure and following creep. As suggested by Chigira (1992) and Deng et al. (2000), a decreasing continuity of rock mass can be attributed to this creep, and lead to the following infiltration of groundwater, the resistivity is thus decreased. Most of the cracks were concentrated in the surface drainage system where the altitude is higher than the shear zone, i.e., in the upper right of profile RIP-1.

Some prospect shear zones may locate on survey lines RIP-1, RIP-2, and RIP-3. The extension of shear zones shown in three RIP sections can be grouped into two directions: one is N20°W; the other is N80°E. These two group shear zones were near the surface and merged together in the vicinity of RIP-1 section. It also extends deeper to the western side of RIP-1 section and separate progressively and obviously, as shown in RIP-2 section and RIP-3 section respectively (Fig. 7). These two shear zones may be two conjugated shear fractures. The acute dihedral angle between them enclosed the maximum principle stress axis, acting in northwest to northwest-by-west direction (Fig. 7). It matches the maximum stress direction in Taiwan.

Long-term monitoring data from wells B13, B13-OW1 and B13-OW2 on the upper slope (Figs. 2 and 7) indicate that the groundwater level remained stable (2041 m, 2063 m and 2062 m a.s.l, respectively). The groundwater surface at the lower part of the slope fluctuated with rainfall. The groundwater above the shear zone is blocked by a natural barrier formed by shear zone; it flows out of shear zone when the water level is higher than the top of shear zone. A tracer test (ITRI, 1993) was carried out in the borehole BH-10 near the well D-1. The

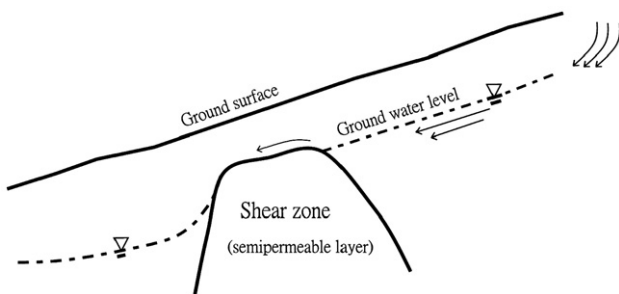


Fig. 8. Map of the hydrogeological model in the study area.

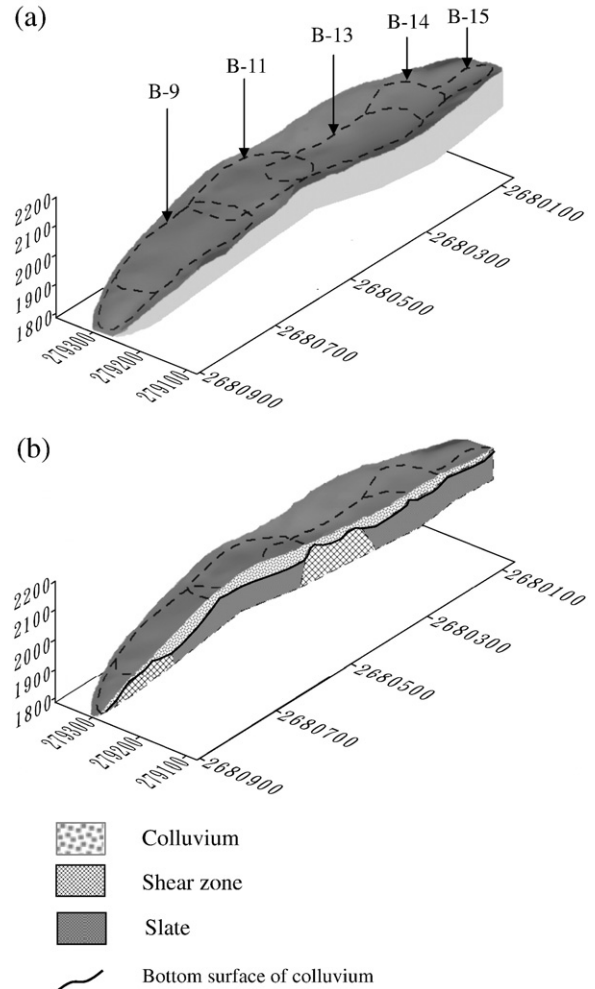


Fig. 9. (a) The 3-D topography of slipping bodies in the study area; (b) A cross section along the central line of slipping bodies shown in (a).

sodium chloride was dropped into the well at a depth of 25.1 to 29 m. The water resistivity decreased first and then increased to a value greater than 1000 Ω-cm within 30 minutes. The result indicates that the groundwater at this depth (around the groundwater level) was in a fast flowing state.

The groundwater table located in the area higher than the shear zone is parallel to the slope surface and has an inclined surface (Fig. 8), unlike a horizontal water surface usually observed in a reservoir. It implies that the recharge groundwater from Fushoushan Farm, blocked by the shear zone, was greater than that of the discharge (Fig. 8). Lai (2000) pointed out that drainage discharge should have additional water source besides precipitation after comparing the water amount difference between precipitation recharge and drainage discharge in the Lishan landslide area. Gravity draws water from the Hehuan River, at a distance of 8 km from the south of the farm, into pools and irrigates the orchards. The irrigation water that infiltrates into the subsurface is the major groundwater resource for the Lishan landslide area. An analyses contents of hydrogen and oxygen isotopes in groundwater indicates there are that 15% derive from precipitation and 85% from Fushoushan Farm

groundwater, the latter may be a major factor controlling landslides in the Lishan area (Peng et al., 2007).

Due to the steep terrain and constructions, it has not been possible to deploy RIP survey lines to detect the extension of shear zone on the southeastern and northwestern side of the landslide body. Nevertheless, as indicated by the studies above, a good continuity of the shear zone can be expected.

Data obtained from the RIP survey lines parallel to the direction of the landslide slippage (RIP-1, RIP-2, RIP-3, RIP-7, and RIP-8) indicate that the bottom of colluvium and clayey fractured slate has curved shapess. It can be confirmed by the planar distribution of slipping bodies from aerial photo (ITRI, 1993), particularly in slipping bodies No. B-9, B-11, B-13, and B-14 (Figs. 2 and 9). Borehole data also shows that a clayey layer fills the gap between the colluvium and undisturbed slate, serving as a slip plane. This circular failure may be associated with the main slope collapse pattern. The study area was about 100 m in width and more than 700 m in length. Such a long and narrow landslide zone is hardly to be formed solely by one landslide event. Moreover, the overlapping of the adjacent slipping body reveals that environmental conditions in situ may have been caused by a sequence of repeated upward-developing landslides (Fig. 9).

## 7. Conclusion

Based on resistivity images and borehole data, the following conclusions can be drawn:

1. The shear zone serves as aquitard, which accumulates groundwater from an upper slope. A sufficient groundwater recharge creates a dynamic balance of groundwater with a stable water level.
2. The extending direction and geometry of shear zones obtained from RIP results can be related to tectonic movement, unlikely to become a slip surface.
3. The RIP results suggest a curved basal surface of colluvium and moisty weathered slate. The landslide was probably formed by a series of repeated retrogressive landslides.
4. There are two ways to stabilize the slope. First, terminate the source of the groundwater, enhance the management of the upper water course and irrigation, and decrease the amount of water permeating into the groundwater. Second, lower the groundwater level by installing drainage wells in the area higher than the shear zone. The northeastern side of RIP-4 may be a proper location.
5. Geological configurations dominate the hydrology of the study site. A combination of RIP data with borehole data does help to discriminate the lithological variation. This study demonstrates that the RIP technique is suitable for this hilly environment.

## 8. Curriculum vitae

### Cheng-Chao Lee

**Date and place of birth:** 01/09/1964; Taipei, Taiwan, R.O.C.

**Sex:** Male

### Current position:

1. 3rd year doctoral student,

Institute of Geophysics, National Central University, Taiwan, ROC

2. Deputy Manager,

Sino Geotechnology, Inc., Taipei, Taiwan, ROC

### Contact:

Institute of Geophysics, National Central University

No. 300, Zhongda, Zhongli City, Taoyuan County 3200, Taiwan, ROC

Tel.: +886 2 25773336x233; fax: +886 2 25785271.

Email: [lcc@sinogeotech.com.tw](mailto:lcc@sinogeotech.com.tw)

### Education qualifications:

1986-1989: Undergraduate studies at the Department of Geology, Chinese Culture University, Taiwan, R.O.C.: Bachelor of Science, honors

1990-1992: Graduate studies for Master of Science at the Institute of Geophysics, National Central University, Taiwan, ROC

### Fields of specialization:

Engineering Geology and Engineering Geophysics

### Professional affiliation:

Geological Society of China

Geophysical Society of China

Engineering Geology technician

### Publications:

Lee, C. C., Chang, J.C., Chen, D. S., 1999. Investigation of the Taipei Fault— A Case Study of Construction Site in Nankang. Central Geological Survey Special Publication No. 11, Special Issue for the Subsurface Geology and Engineering Environment of Taipei Basin, 182-205. (Abstract in English)

Lee, C. C., Yu, C. Han., Chou, C. C., 2003. Case Study of Geological Investigation and Seismic Evaluation of Site Near Churlungpu Fault. The 10th Conference on Current Researches in Geotechnical Engineering in Taiwan.

## Acknowledgements

We are grateful to Dr. D. S. Chen, the ex-board chairman of Sino Geotechnology (Sino Geotech) Inc, sorrowful, who passed away on 2007/10/15, for he generously provided both boring and monitoring data for this study. We thank the engineers at Sino Geotech for help with the fieldwork. The authors would like to express deep thanks to the editor and reviewers for their constructive comments. Prof. Louis L. Tsai and M. L. Lin are highly appreciated for devoting time to discussions and suggestions.

## References

- Turesson, Anita, 2006. Water content and porosity estimated from ground-penetrating radar and resistivity. *Journal of Applied Geophysics* 58, 99–111.
- Nascimento da Silva, Carlos César, de Medeiros, Walter Eugênio, Jardim de Sá, Emanuel Ferraz, Neto, Pedro Xavier, 2006. Resistivity and ground-penetrating radar images of fractures in a crystalline aquifer: a case study in Caiçara farm—NE Brazil. *Journal of Applied Geophysics* 58, 144–157.
- Chigira, M., 1992. Long-term gravitational deformation related to the toppling of rocks by mass rock creep. *Engineering Geology* 32, 157–184.

- China Engineering Consultants Incorporation (ITRI), 1997. Investigation and remediation plans(I) for the Lishan landslide area. Report to the Soil and Water Conservation Bureau, Taiwan.
- Deng, Q.L., Zhu, Z.Y., Chu, Z.Q., Wang, X.P., 2000. Mass rock creep and landsliding on the Huangtupo slope in the reservoir area of the Three Gorges Project, Yangtze River, China. *Engineering Geology* 58, 67–83.
- Šumanovac, Franjo, Weisser, Mario, 2001. Evaluation of resistivity and seismic methods for hydrogeological mapping in karst terrains. *Journal of Applied Geophysics* 47, 13–28.
- Šumanovac, Franjo, 2006. Mapping of thin sandy aquifers by using high resolution reflection seismics and 2-D electrical tomography. *Journal of Applied Geophysics* 58, 144–157.
- Griffiths, D.H., Barker, R.D., 1993. Two-dimensional resistivity imaging and modelling in areas of complex geology. *Journal of Applied Geophysics* vol. 29, 211–226.
- Ho, C.S., 1986. An introduction to the geology of Taiwan, Explanatory text of the geologic map of Taiwan, (2nd ed.). M.O.E.A., ROC.
- Industrial Technology Research Institute (ITRI), 1993. Investigation and Remediation Plans(I) for Lishan Landslide Area. Taiwan, Report to the Soil and Water Conservation Bureau.
- Porsani, Jorge Luís, Elis, Vagner Roberto, Hiodo, Francisco Yukio, 2005. Geophysical investigations for the characterization of fractured rock aquifers in Itu, SE Brazil. *Journal of Applied Geophysics* 57, 119–128.
- Lai, T.C., 2000. The role of geological investigation in the planning or design a landslide stabilizing measurement—case study of Lishan landslide stabilization. Paper presented at proceedings of the second national conference on landslide stabilization and disaster prevention in Taiwan. 16–18 February 2000 (in Chinese with English abstract).
- Lapenna, V., Lorenzo, P., Perrone, A., Piscitelli, S., Rizzo, E., Sdao, F., 2004. 2D electrical resistivity imaging of some complex landslides in the Lucanian Apennine chain, southern Italy. *Geophysics* 70, B11–B18.
- Loke, M.H., Barker, R.D., 1996. Rapid least-squares inversion of apparent resistivity pseudosections by a quasi-Newton method. *Geophysical Prospecting* vol. 44, 499–524.
- Loke, M.H., 2001. Tutorial: 2-D and 3-D Electrical Imaging Surveys. [www.goelectrical.com](http://www.goelectrical.com).
- Mauritsch, H.J., Seiberl, W., Arndt, R., Romer, A., Schneiderbauer, K., Sendlhofer, G.P., 2000. Geophysical investigations of large landslides in the Carnic region of southern Austria. *Engineering Geology* 56, 373–388.
- Peng, T.R., Wang, C.H., Lai, T.C., Ho, S.K., 2007. Using hydrogen, oxygen, and tritium isotopes to identify the hydrological factors contributing to landslides in a mountainous area, central Taiwan. *Environmental Geology* 52, 1617–1629.
- Perrone, A., Iannuzzi, A., Lapenna, V., Lorenzo, P., Piscitelli, S., Rizzo, E., Sdao, F., 2004. High-resolution electrical imaging of the Varco d', Izzo earthflow (southern Italy). *Journal of Applied Geophysics* 56, 17–29.
- Gautam, Pitambar, Raj Pant, Surendra, Ando, Hisao, 2000. Mapping of subsurface karst structure with gamma ray and electrical resistivity profiles: a case study from Pokhara valley, central Nepal. *Journal of Applied Geophysics* 45, 97–110.
- Sino Geotechnology Incorporation (Sino Geotech), 2001. Analysis and application of Monitoring system for Lishan Landslide Area (in Chinese). Report to the Soil and Water Conservation Bureau, Taiwan.
- Sino Geotechnology Incorporation (Sino Geotech), 2003. Geological records of excavated G1 & G2 drainage gallery in Lishan Landslide Area, Taiwan (in Chinese; unpublished).
- Soil and Water Conservation Bureau (SWCB), 2003. A pictorial guide of remediation plans for Lishan landslides (Abstract in English), Taiwan.
- Su, T.R., Liu, M.F., Su, C.L., 1990. Investigation of remediation of slope stability in E-W Crossing-Island Highway (in Chinese): Report of disaster prevention technology to NSC, ROC, No. 75-10.
- Tsai, Y.B., Liaw, Z.S., Lee, T.Q., Lin, M.T., Yeh, Y.H., 1981. Seismological evidence of an active plate boundary in the Taiwan area. *Memoir - Geological Society of China* 4, 143–154.
- Yaramanci, Ugur, Lange, Gerhard, Hertrich, Marian, 2002. Aquifer characterisation using Surface NMR jointly with other geophysical techniques at the Nauen/Berlin test site. *Journal of Applied Geophysics* 50, 47–65.
- Karastathis, V.K., Karmis, P.N., Drakatos, G., Stavrakakis, G., 2002. Geophysical methods contributing to the testing of concrete dams, Application at the Marathon Dam. *Journal of Applied Geophysics* 50, 247–260.
- Wan, H.M., 1986. Study the relationship between the clayey mineral and the slope failure of colluvial soils along E-W Cross-Island Highway (in Chinese). Report of disaster prevention technology to NSC, ROC. No. 75–52.
- Yu, H.M., Chen, H.Y., 1994. Global positioning system measurement of crustal deformation in the Taiwan arc-continent collision zone. *Terrestrial Atmospheric and oceanic Sciences* 5, 477–498.
- Yu, H.M., Kuo, L.C., Punongbayan, R.S., Ramos, E.G., 1999. GPS observations of crystal deformation in the Taiwan-Luzon region. *Geophysical Research Letters* 26, 923–926.